Received: 24 September 2018 | Revised: 10 May 2019 | Accepted: 28 May 2019

DOI: 10.1002/jcp.28966

ORIGINAL RESEARCH ARTICLE

Journal of Cellular Physiology WILEY

Autophagy induces eosinophil extracellular traps formation and allergic airway inflammation in a murine asthma model

Josiane Silva Silveira[1] | Géssica Luana Antunes[1] | Daniela Benvenutti Kaiber[1] | Mariana Severo da Costa[1] | Fernanda Silva Ferreira[2] | Eduardo Peil Marques[2] | Felipe Schmitz[2] | Rodrigo Benedetti Gassen[3] | Ricardo Vaz Breda[4] | Angela T. S. Wyse[2] | Renato Tetelbom Stein[1] | Paulo Márcio Pitrez[1] | Aline Andrea da Cunha[1]

[1]Laboratory of Pediatric Respirology, Infant Center, School of Medicine, Pontifical Catholic University of Rio Grande do Sul, Porto Alegre, Rio Grande do Sul, Brazil

[2]Laboratory of Neuroprotection and Neurometabolic Disease, Department of Biochemistry, Federal University of Rio Grande do Sul, Porto Alegre, Rio Grande do Sul, Brazil

[3]Laboratory of Cellular and Molecular Immunology, School of Science, Pontifical Catholic University of Rio Grande do Sul, Porto Alegre, Rio Grande do Sul, Brazil

[4]School of Medicine, Instituto do Cérebro do Rio Grande do Sul, Pontifical Catholic University of Rio Grande do Sul, Porto Alegre, Rio Grande do Sul, Brazil

Correspondence
Aline Andrea da Cunha, Laboratory of Pediatric Respirology, Infant Center, School of Medicine, Pontifical Catholic University of Rio Grande do Sul, 6690 Ipiranga Ave., 2nd floor, Room 13, Porto Alegre – RS 90610-000 Brazil.
Email: alineacunha@hotmail.com

Abstract

Studies have shown autophagy participation in the immunopathology of inflammatory diseases. However, autophagy role in asthma and in eosinophil extracellular traps (EETs) release is poorly understood. Here, we attempted to investigate the autophagy involvement in EETs release and in lung inflammation in an experimental asthma model. Mice were sensitized with ovalbumin (OVA), followed by OVA challenge. Before the challenge with OVA, mice were treated with an autophagy inhibitor, 3-methyladenine (3-MA). We showed that 3-MA treatment decreases the number of eosinophils, eosinophil peroxidase (EPO) activity, goblet cells hyperplasia, proinflammatory cytokines, and nuclear factor kappa B (NFκB) p65 immunocontent in the lung. Moreover, 3-MA was able to improve oxidative stress, mitochondrial energy metabolism, and Na^+, K^+-ATPase activity. We demonstrated that treatment with autophagy inhibitor 3-MA reduced EETs formation in the airway. On the basis of our results, 3-MA treatment can be an interesting alternative for reducing lung inflammation, oxidative stress, mitochondrial damage, and EETs formation in asthma.

KEYWORDS

asthma, autophagy, eosinophil extracellular traps, eosinophils, inflammation

1 | INTRODUCTION

Asthma is an inflammatory disease that enhances inflammatory cells, mucus production, remodeling, and inflammatory mediators in the airway, which may cause impairment in lung function (Lambrecht & Hammad, 2015). Granulocytes such as eosinophils participate in asthma immunopathology. Eosinophil granule proteins contain eosinophil peroxidase (EPO), which is related to the inflammation and injury in the lung (Sanz, Parra, Prieto, Dieguez, & Oehling,1997). Besides, asthma induces oxidative stress due to a reduction in antioxidant defense mechanisms and increase in reactive oxygen species (ROS) formation being associated to damage to biologic molecules in airway and impairment in lung function (Comhair & Erzurum, 2010; Cunha et al., 2016). Oxidative stress also causes an

Abbreviations: 3-MA, 3-methyladenine; AHR, airway hyperresponsiveness; AKT, protein kinase B; ATG5, autophagy-related gene 5; AVOs, acidic vesicle organelles; BALF, bronchoalveolar lavage fluid; BSA, bovine serum albumin; CAT, catalase; DCIP, 2,6-dichloroindophenol; DCF, dichlorofluorescein; DPBS, Dulbecco's phosphate buffered-saline; EETs, eosinophil extracellular traps; EPO, eosinophil peroxidase; FBS, fetal bovine serum; G, tissue damping; GPx, glutathione peroxidase; H, tissue elastance; H2DCF-DA, 2′7′ dichlorofluorescein diacetate; H&E, hematoxylin and eosin; IFN, interferon; IgE, immunoglobulin E; IL, interleukin; LC3B, light chain 3B; NADPH, nicotinamide adenine dinucleotide phosphate; NFκB, nuclear factor kappa B; OVA, ovalbumin; PBS, phosphate-buffered saline; PFA, paraformaldehyde; PI, propidium iodide; Rn, resistance; ROS, reactive oxygen species; SDH, succinate dehydrogenase; SOD, superoxide dismutase; TNF-α, tumor necrosis factor α.

 © 2019 Wiley Periodicals, Inc.

important mitochondrial dysfunction and inactivation of the electron transport chain in the lung (Mabalirajan et al., 2008).

Autophagy is a crucial intracellular mechanism, by which injury proteins and organelles are captured to autophagosomes and taken to lysosomes for deterioration to keep cell survival during cellular stress and starvation (Mizushima, 2007). Studies have shown autophagy participation in immunity and in inflammatory disease (Jyothula & Eissa, 2013; Poon, Eidelman, Laprise, & Hamid., 2012). Ban et al. (2015) observed an increase in autophagosomes number in sputum cells and in peripheral blood cells in asthmatic patients. Recently, some studies observed the relation between genetic polymorphisms of autophagy-related gene 5 (ATG5) and asthma (Martin et al., 2012; Poon et al., 2012). Liu et al. (2016) demonstrated that autophagy inhibition significantly decreased lung eosinophilia, inflammation, interleukin 5 (IL-5) levels, and airway hyperresponsiveness (AHR) in ovalbumin (OVA)-challenged mice. However, autophagy role in asthma immunopathology is still poorly understood.

In 2008, Yousefi et al. (2008) reported by the first time DNA extracellular traps release by eosinophils. Eosinophil extracellular traps (EETs) are constituted by extracellular DNA and intact eosinophil granules that trap microorganisms (Ueki et al., 2016; Yousefi et al., 2008). EETs release is an important mechanism of the inflammatory response in allergic diseases (Simon et al., 2011; Ueki et al., 2016). Dworski, Simon, Hoskins, & Yousefi (2011) showed EETs formation in the airway of asthmatic patients. Furthermore, Cunha et al. (2014) observed EETs formation in the airway in asthmatic mice. EETs release may increase immunopathology of asthma, even though EETs mechanisms have not been elucidated. Evidence has shown that autophagy regulates the process of extracellular traps release by neutrophils (Kenno et al., 2016; Remijsen et al., 2011). Pham et al. (2017) verified positive correlations between neutrophil extracellular traps formation and autophagy in peripheral blood in asthmatic patients. However, autophagy participation in the mechanism of EETs formation is not broadly understood.

Although autophagy plays a crucial role in inflammatory disease (Puleston & Simon, 2014), there is little knowledge of its mechanisms in asthma and in EETs formation. Here, we analyzed the outcome of an autophagy inhibitor, 3-methyladenine (3-MA), in EETs formation and in lung inflammation in asthmatic mice. We have chosen 3-MA because it is an important autophagy inhibitor, which blocks autophagosome formation. Our study hypothesized that autophagy enhancement in eosinophils increases EETs formation and inflammation in the airway in asthmatic mice.

2 | MATERIALS AND METHODS

2.1 | Animals

We used 6–8 week old specific-pathogen-free female BALB/cJ mice weighing approximately 20 g. They were acquired from the Center for Experimental Biological Models (Porto Alegre, Brazil) and kept with ration and water ad libitum on a 12:12 hr light–dark cycle. The experimental protocols were approved in the Pontifical Catholic University of Rio Grande do Sul (Porto Alegre, Brazil) by the Animal Ethics Committee (#7910) and all mice care followed the "Guide for the Care and Use of Laboratory Animals."

2.2 | Experimental asthma and 3-MA treatment protocol

Mice were sensitized subcutaneously with OVA (20 μg) (Grade V; Sigma) on Days 0 and 7. Next, mice were challenged intranasally with OVA (100 μg) on Days 14, 15, and 16 (Cunha et al., 2016). The negative control group received subcutaneous and intranasal Dulbecco's phosphate buffered-saline (DPBS; Gibco). To investigate the participation of autophagy in EETs release, we used an autophagy inhibitor, 3-MA (Sigma). Autophagy inhibitor 3-MA blocks a crucial protein, Type III phosphatidylinositol 3-kinases, for the onset of autophagy. The treatment was performed 45 min before the three intranasal challenges, with intranasal administration of 15 mg/kg of 3-MA (Liu et al., 2016).

2.3 | Total and differential cell counts in bronchoalveolar lavage fluid

On Day 17 of the protocol, first the mice were anesthetized (xylazine 0.2 mg/g and ketamine 0.4 mg/g) and bronchoalveolar lavage fluid (BALF) was collected with 1 ml of phosphate-buffered saline (PBS; Gibco) and 2% fetal bovine serum (FBS). BALF was centrifuged and cells were diluted in PBS with 2% FBS for performing total cell counts and differential cell counts. The total cell counts were determined by Trypan blue exclusion method in a hemocytometer (Neubauer chamber). Differential cell counts were done by cytospin preparations (Eppendorf) and stained with hematoxylin and eosin (H&E) (Newprov). Four hundred cells were counted using an optical microscope Olympus BX43 (Olympus, Tokyo, Japan).

2.4 | Analysis of the activity of EPO in BALF

BALF supernatant was incubated with working reagent (0.1 mM *O*-phenylenediamine (Sigma), 0.05 M Tris, Triton X-100, and 1 mM hydrogen peroxide, pH 8.0). Afterward, the reaction was finished with sulfuric acid 1.0 M. The absorbance was evaluated in a spectrophotometer at 492 nm (Strath, Warren, & Sanderson, 1985).

2.5 | Lung histology

Lungs were perfused with 10% buffered formalin for histological and morphological analysis. Lungs were included in paraffin blocks and cut into 50-μm sections. Inflammatory infiltrate was analyzed by H&E dye. To evaluate the extent of perivascular and peribronchial inflammatory cells infiltrate in μm, 10 measurements were performed starting from the beginning of the bronchial or vessel epithelium to the end of the inflammatory cells infiltrate using

Olympus CellSens Standard software (Olympus). Mucus production and goblet cells hyperplasia were evaluated by Alcian blue dye.

2.6 | Assessment of respiratory system mechanics

The mice were anesthetized (ketamine 0.4 mg/g and xylazine 0.2 mg/g) on Day 17 of the protocol. Respiratory system mechanics testing was performed after cannulation of the trachea and the mice were connected to FlexiVent (SCIREQ). Three measurements of forced oscillation technique were performed during a pause of the respirator (3 s). During the ventilation pauses, a frequency oscillatory signal (4–38 Hz) was created by a loudspeaker and passed through the tracheal cannula of the animal. Newtonian resistance (Rn) is equivalent to airway resistance in mice due to the complacency of the chest wall. Tissue damping (G) analyzes the resistance of small airways whereas tissue elastance (H) represents the energy conservation in the alveolus. The data were analyzed in a specific software (FlexiWare, SCIREQ), where airway resistance and elastic properties (viscosity and elasticity) of the lung were measured through a pulmonary impedance (Hantos et al., 1992; Zosky et al., 2008).

2.7 | Cytokine levels in lung

Lung samples were macerated in PBS 1X and IL-5, IL-13, interferon γ (IFN-γ), IL-1β, tumor necrosis factor α (TNF-α), and IL-10 were measured by multiplex assay according to the manufacturer's recommendations using a Milliplex MAP mouse kit (MILLIPLEX®, Millipore) and Procarta Plex Multiplex immunoassay (Thermo Fisher Scientific). Results were analyzed using the xPONENT® Solutions software (Luminex Corporation).

2.8 | Lung preparation

For oxidative stress analyses (ROS, superoxide dismutase [SOD], catalase [CAT], and glutathione peroxidase [GPx]) in lungs, the samples were macerated (1:10, wt/vol) in 140 mM potassium chloride 20 mM sodium phosphate. For mitochondrial energy metabolism analyses, lungs were frozen and thawed three times to disrupt the mitochondrial membranes. After lungs were macerated (1:20, wt/vol) in 10 mM Trizma base, 2 mM ethylenediaminetetraacetic acid (EDTA), 50 UI/ml heparin, and 250 mM sucrose, pH 7.4. For NA^+, K^+-ATPase activity analysis, lungs were macerated (1:10, wt/vol) in 0.32 mM sucrose, 5.0 mM hydroxyethyl piperazineethanesulfonic acid, and 1.0 mM EDTA, pH 7.5. Afterward, the samples were then centrifuged (10 min at 800 g) and the supernatant was stored.

2.9 | ROS assay in lung

ROS production was analyzed by the colorimetric assay based in the oxidation of the 2′7′ dichlorofluorescein diacetate (H2DCF-DA). The lung supernatants were incubated in 100 μM H2DCF-DA and dichlorofluorescein (DCF) were analyzed at 488 nm of excitation and 525 nm of emission in a spectrophotometer. The ROS levels were expressed as DCF nmol/mg protein (LeBel et al., 1992).

2.10 | GPx activity in lung

The lung supernatants were incubated in 0.1 mM nicotinamide adenine dinucleotide phosphate (NADPH), 0.15 U/ml glutathione reductase, 2 mM glutathione, 0.4 mM sodium azide, and 0.5 mM tert-butyl hydroperoxide. The decay of the NADPH was analyzed at 340 nm in a spectrophotometer. One GPx unit was defined as 1 μmol of NADPH metabolized per minute. GPx was plotted in GPx units/mg of protein (Wendel, 1981).

2.11 | SOD activity in lung

The SOD activity was analyzed according to Marklund (1985). SOD inhibits pyrogallol autoxidation, and its activity can be indirectly analyzed in a spectrophotometer at 420 nm. The standard curve was performed with purified SOD. SOD was plotted in units of SOD/mg protein.

2.12 | CAT activity in lung

The lung samples were added to a buffer containing 0.1% of Triton X-100, 10 mM potassium phosphate, and 20 mM hydrogen peroxide. The consume of the hydrogen peroxide was evaluated in a spectrophotometer at 240 nm. One CAT unit was defined as 1 mM of hydrogen peroxide consumed per minute. CAT was reported as units of CAT/mg protein (Aebi, 1984).

2.13 | Complex II, succinate dehydrogenase, and Complex IV activity in lung

Lung samples were incubated in 8 mM 2,6-dichloroindophenol (DCIP), 16 mM sodium succinate, and 40 mM potassium phosphate. Next, 40 mM DCIP, 4 mM sodium azide, and 7 mM rotenone were added. Complex II in the lung was analyzed after reduction of the DCIP. Succinate dehydrogenase (SDH) was analyzed after the decrease of the absorbance by the reduction of the DCIP with phenazine methosulfate. The absorbance was analyzed at 600 nm in a spectrophotometer and the data were plotted as nmol/minute/mg of protein (Fischer et al., 1985). Complex IV was analyzed after to oxidation of previously reduced cytochrome c. Supernatants were incubated in 7 μg of cytochrome c, 10 mM potassium phosphate, and 0.6 mM n-dodecyl-β-*D*-maltoside. The absorbance was analyzed at 550 nm. Complex IV was plotted as nmol/minute/mg of protein (Rustin et al., 1994).

2.14 | NA^+, K^+-ATPase activity in lung

NA^+, K^+-ATPase was analyzed according to Wyse et al. (2000). Lung samples were incubated in 5.0 mM magnesium chloride, 80.0 mM sodium chloride, 20.0 mM potassium chloride, 40.0 mM

Tris-hydrochloric acid (HCl), and 3.0 mM adenosine triphosphate, pH 7.4. Controls were added 1.0 mM of ouabain. The results were plotted as nmol of inorganic phosphate released per min/mg of protein.

2.15 | Quantification of extracellular DNA traps and immunofluorescence in BALF eosinophils

Extracellular DNA levels in BALF supernatant was determined by the Quant-iT dsDNA HS kit (Invitrogen). To visualize the EETs formation by immunofluorescence microscopy, BALF eosinophils (2×10^5/ml) were plated in eight-chamber culture slides and incubated at 37°C with 5% carbon dioxide for 1 hr. Afterward, BALF eosinophils were incubated with 4% paraformaldehyde (PFA) for 45 min. Next BALF eosinophils were incubated for 45 min with primary antibodies, anti-EPO and anti-histone H2B (1:250; Santa Cruz Biotechnology). After this time, BALF eosinophils were incubated with secondary antibodies for 30 min, fluorescein isothiocyanate (FITC) anti-goat (1:100; Santa Cruz Biotechnology) and Alexa fluor 633 anti-goat (1:100 in PBS, Invitrogen). Finally, the BALF eosinophils were stained for 4 min with Hoechst 33342 DNA dye (1:2000, Invitrogen). Images were performed in a Zeiss LSM5 Exciter confocal microscope (Zeiss LSM5).

2.16 | Analysis of cell death in BALF eosinophils

BALF eosinophils were analyzed for apoptosis and necrosis by Annexin-V and propidium iodide (PI; BD Biosciences). The Samples were incubated in buffer containing Annexin-V-FITC (5 µl) and PI (5 µl) for 15 min according to the manufacturer's instructions and determined by flow cytometry (FACS Canto II, BD Biosciences). Results were evaluated using FlowJo software version X.0.7 (TreeStar, OR).

2.17 | Analysis of light chain 3B and protein kinase B in the lung by Western blot

Lungs were homogenized in lysis solution (10 mM Tris-HCl, 1 mM magnesium chloride, 0.1 mM phenylmethylsulfonyl fluoride 10%, glycerol 2.1 mM EDTA, 5 mM β-mercaptoethanol, and 0.5% 3-[(3-cholamidopropyl) dimethylammonio]-1-propanesulfonate, pH 7.5). Proteins (20 µg) were separated in polyacrylamide gel (10%) by electrophoresis. Proteins were transferred to a nitrocellulose membrane (GE Healthcare Life Sciences, PA) and it was blocked with blocking buffer (bovine serum albumin [BSA] 5% in TBST). Afterward, the blot was incubated with anti-light chain 3B (LC3B; 1:200 in BSA; Thermo Fisher Scientific), anti-protein kinase B (AKT; 1:500 in

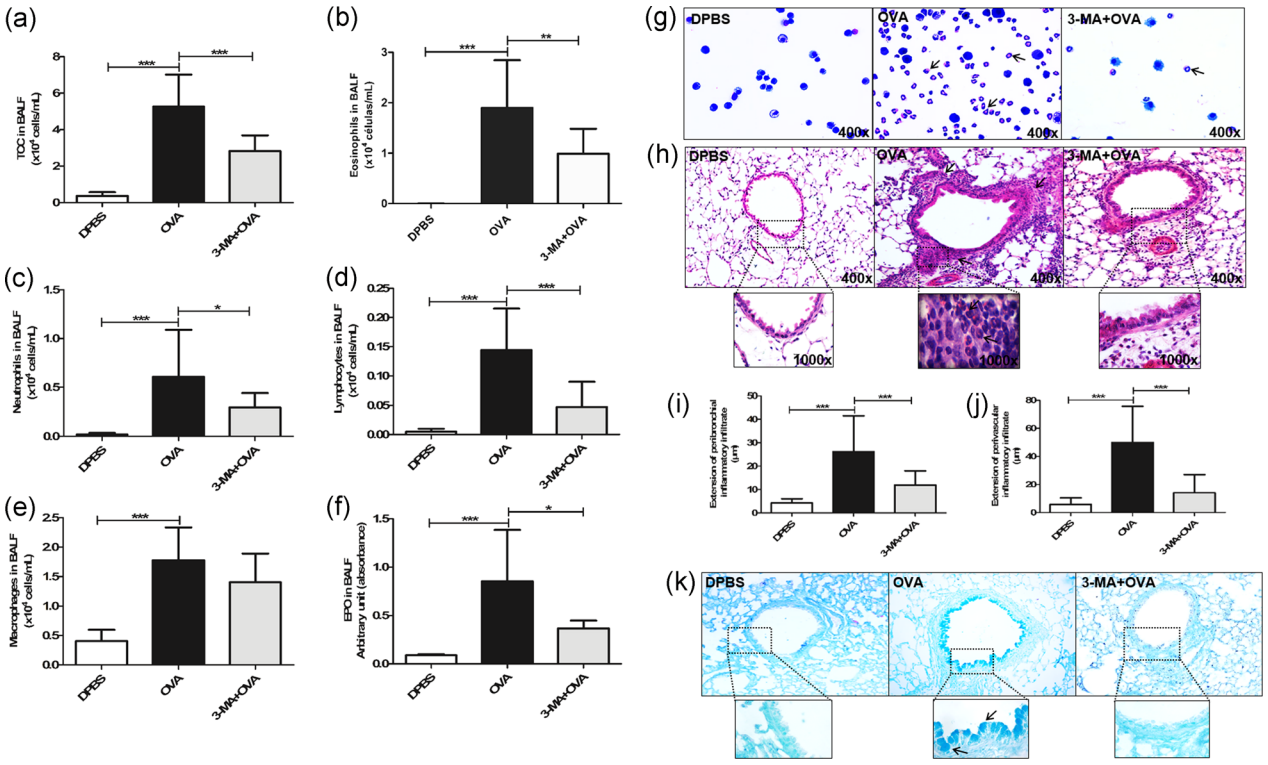

FIGURE 1 3-MA reduces inflammation, EPO activity, and goblet cells hyperplasia in airways. (a) Total cell counts in BALF. (b–e) Differential cell counts in BALF (eosinophils, neutrophils lymphocytes, and macrophages. (g) Representative illustration of BALF cells stained with H&E (×400 magnification, arrows indicate eosinophils). (f) Analysis of the activity of the EPO enzyme in BALF. (h) Histopathological analysis in the lung. Representative photomicrographs of lung sections stained with H&E (×200 and ×1,000 magnification, arrow indicate inflammatory infiltrate). (i–j) Morphometric analysis perivascular and peribronchial with H&E staining. (k) Representative photomicrographs of sections stained with alcian blue (×200 and ×1,000 magnification, arrows indicate goblet cells). Data represent the mean ± *SD*, *n* = 10 animals per group. 3-MA, 3-methyladenine; ANOVA, analysis of variance; BALF, bronchoalveolar lavage fluid; DPBS, Dulbecco's phosphate buffered-saline; EPO, eosinophil peroxidase; H&E, hematoxylin, and eosin; OVA, ovalbumin; *SD*, standard deviation. *$p < .05$, **$p < .01$, and ***$p < .001$ (one-way ANOVA followed by Tukey's test) [Color figure can be viewed at wileyonlinelibrary.com]

BSA 5%; Cell Signaling Technology), or anti-β-Actin (1:1000 in BSA 5%; Cell Signaling Technology) overnight. Finally, it was incubated with secondary antibody, horseradish peroxidase anti-rabbit (1:1000 in BSA 5%; Cell signaling). The blot was developed using a Chemiluminescent photo finder (Kodak/Carestream). The bands were normalized by β-actin using Image J (Rueden et al., 2017).

2.18 | Detection and quantification of acidic vesicle organelles in BALF eosinophils

Acidic vesicle organelles (AVOs) formation was analyzed using acridine orange (AO; Sigma) dye, which emits green fluorescence in the nucleus and cytoplasm and red fluorescence in the AVOs formation. BALF eosinophils (2×10^5/ml) were plated in eight-chamber culture slides and stained with the AO (1 μg/ml) for 15 min. Images were performed in a confocal microscope (Zeiss LSM5). To quantify AVOs, BALF eosinophils were incubated with AO (1 μg/ml) and were determined by flow cytometry (FACS Canto II, BD Biosciences). We analyzed the data by the FlowJo software version X.0.7 (TreeStar).

2.19 | Analysis of nuclear factor kappa B (NFκB) p65 and LC3B proteins in the lung by immunofluorescence

First, lung slices were incubated with 10 mM citrate (pH 9.0) for 10 min, 1% hydrogen peroxide in methanol for 20 min followed by 10% BSA for 30 min. After that, slices were incubated with anti-NFκBp65 or anti-LC3B (1:500; Santa Cruz Biotechnology) for 40 min, followed by secondary antibody, FITC anti-rabbit (1:250; Santa Cruz Biotechnology) for 30 min. Finally, Hoechst 33342 (1:2000; Invitrogen) was added for 4 min. Images were examined with a confocal microscope (Zeiss LSM5).

2.20 | Analysis of LC3B in BALF cells by immunofluorescence

BALF eosinophils (2×10^5/ml) were plated in eight-chamber culture slides and incubated with 4% PFA for 15 min. Afterward, the eosinophils were permeabilized with Triton X-100 (0.1%) for 15 min and incubated with anti-LC3B (0.5 μg/ml; Invitrogen) primary antibody for 1 hr, followed by incubation for 40 min with secondary antibody, FITC anti-rabbit (1:100; Thermo Fisher Scientific). Afterward, eosinophils were stained for 4 min with Hoechst 33342 dye (1:2000; Invitrogen) and visualized by confocal microscope Zeiss LSM5 Exciter (Zeiss LSM5, Oberkohen, Germany).

2.21 | Protein levels determination in lung

The proteins content in lungs were determined using the Qubit™ Protein Assay Kit (Invitrogen) for cytokines analyses. Lowry assay for proteins from oxidative stress and mitochondrial energy metabolism (Lowry, Rosebrough, Farr, & Randall, 1951). In accordance to Bradford (1976) for proteins from the western blot and Na^+, K^+-ATPase.

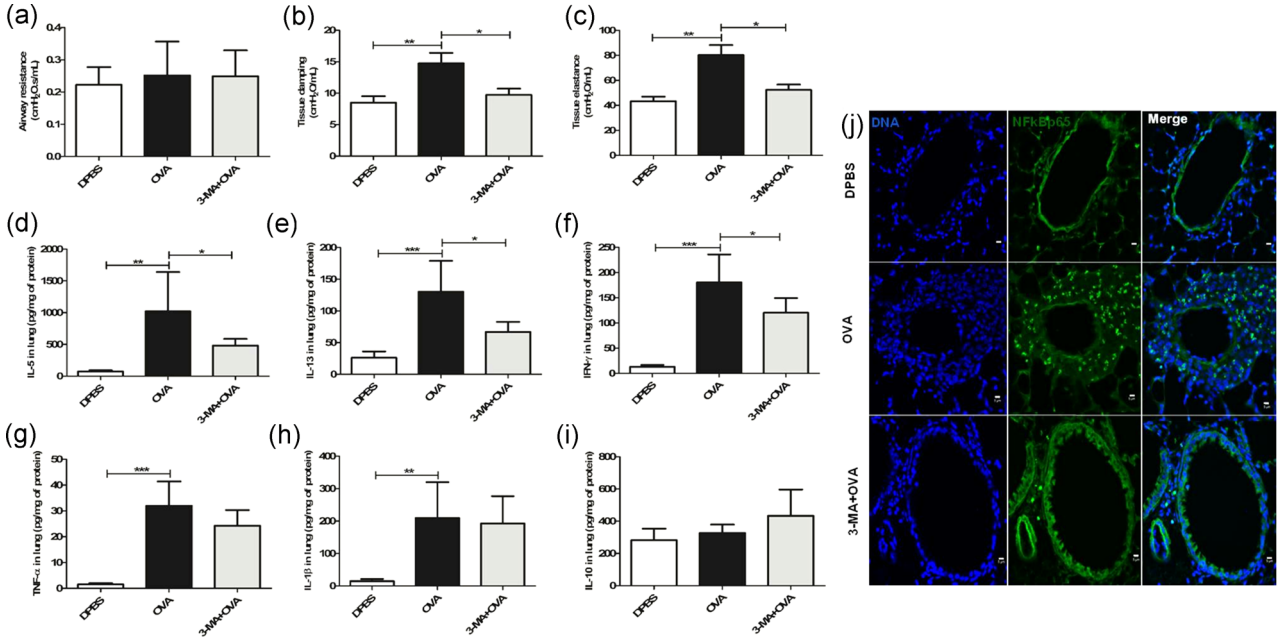

FIGURE 2 3-MA improves respiratory system mechanics, decreases inflammatory cytokines, and NFκB p65 in lung. (a–c) Assessment of respiratory system mechanics: resistance (Rn), tissue damping (G), and tissue elastance (H). (d–i) Cytokine levels in lung (IL-5, IL-13, IFN-γ, IL-1β, TNF-α, and IL-10). (j) Analysis of the NFκB p65 protein by immunofluorescence in lung (×630 magnification, scale bars = 5 μm). Lung sections were incubated with anti-NFκB p65, followed by incubation with secondary antibody, FITC anti-rabbit. Lung sections were stained with Hoechst 33342 and visualized by confocal microscopy. Data represent the mean ± *SD*, *n* = 10 animals per group. 3-MA, 3-methyladenine; ANOVA, analysis of variance; DPBS, Dulbecco's phosphate buffered-saline; FITC, fluorescein isothiocyanate; IFN-γ, interferon γ; IL-5, interleukin 5; NFκB, nuclear factor kappa B; OVA, ovalbumin; *SD*, standard deviation; TNF-α, tumor necrosis factor α. $^*p < .05$, $^{**}p < .01$, and $^{***}p < .001$ (One-way ANOVA followed by Tukey's test) [Color figure can be viewed at wileyonlinelibrary.com]

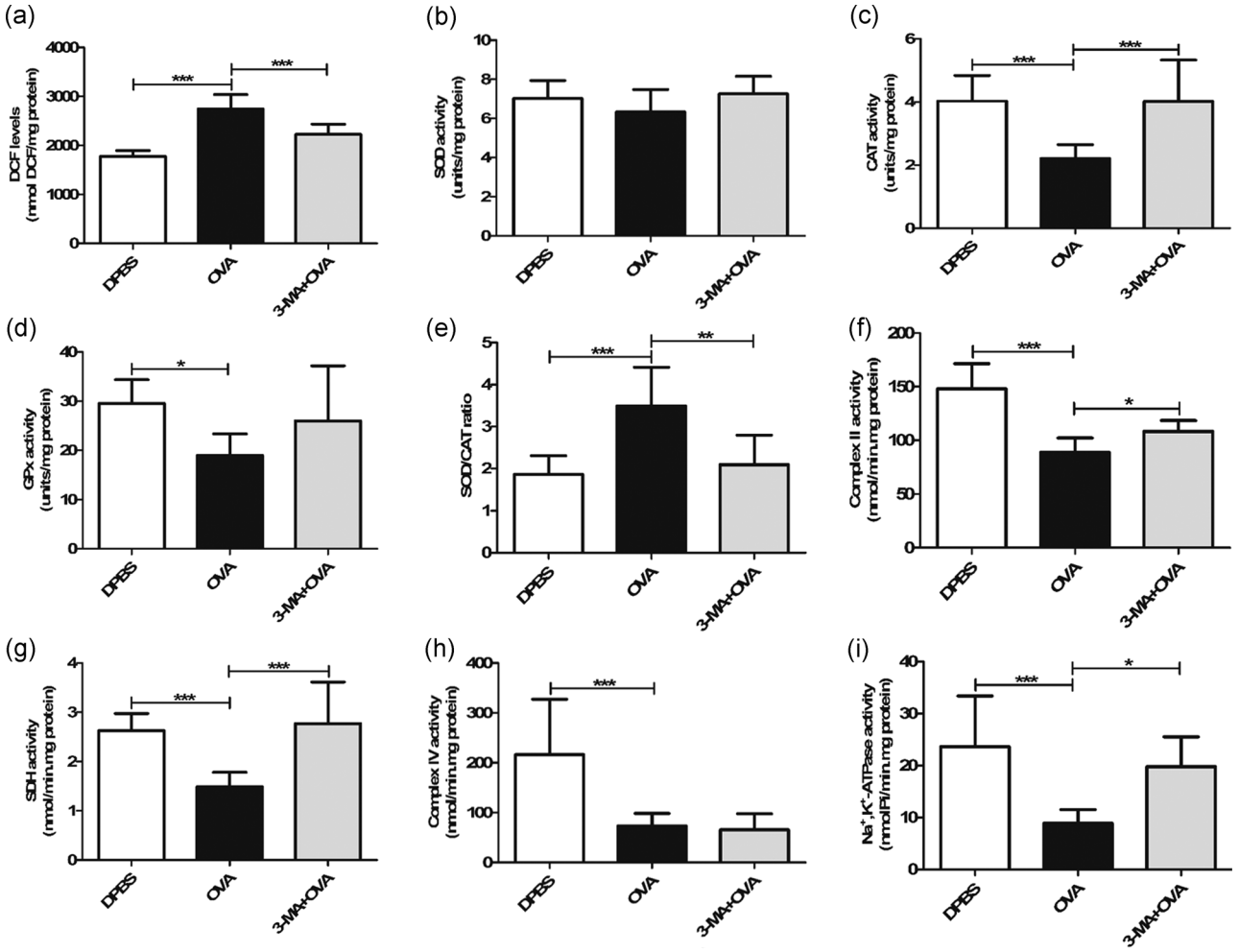

FIGURE 3 3-MA decreases oxidative stress, improves mitochondrial energy metabolism, and NA+, K+-ATPase activity in the lung. (a) ROS production in the lung. (b–e) Activities of antioxidant enzymes (SOD, CAT, and GPx) in the lung. (f–h) Mitochondrial energy metabolism (Complex II, SDH, and Complex IV) analysis in the lung. (b–e) NA+, K+-ATPase activity in the lung. Data represent the mean ± *SD*, *n* = 10 animals per group. 3-MA, 3-methyladenine; ANOVA, analysis of variance; CAT, catalase; DCF, dichlorofluorescein; DPBS, Dulbecco's phosphate buffered-saline; GPx, glutathione peroxidase; OVA, ovalbumin; ROS, reactive oxygen species; *SD*, standard deviation; SDH, succinate dehydrogenase; SOD, superoxide dismutase. **p* < .05, ***p* < .01, and ****p* < .001 (one-way ANOVA followed by Tukey's test)

2.22 | Statistical analysis

Data were expressed as mean ± standard deviation. The Shapiro–Wilk normality test was used to evaluate the normal distribution of the data. We used analysis of variance followed by Tukey's pos-hoc and the adopted significance level was $p \leq .05$. Statistical analysis and graphs were performed using the GraphPad Prism Software, version 5 (GraphPad Software, San Diego).

3 | RESULTS

3.1 | 3-MA reduces inflammation, EPO activity, and goblet cells hyperplasia in airways

We analyzed airway inflammation to evaluate the development of an experimental asthma model. We observed that the OVA group had a significant increase in the total cell counts, as well as an increase in eosinophils, neutrophils, macrophages, and lymphocytes counts when compared with the control group. We also verified the ability of 3-MA in decreasing pulmonary inflammation. 3-MA-treated OVA group showed a decrease in total cell counts as well as a decrease in eosinophils and neutrophils counts in BALF compared with the OVA group (Figure 1a–e,g). We evaluated whether the 3-MA treatment was capable of to decrease eosinophil granule protein EPO in BALF. In EPO activity analysis, we demonstrated that OVA significantly increased the levels of EPO in BALF whereas 3-MA administration decreased significantly EPO activity (Figure 1f). Then, we decided to investigate whether 3-MA would be able to prevent the induction of histopathological changes in the lung. In the histopathological analysis, we demonstrated an increase in inflammatory cells infiltration located in peribronchial and perivascular areas in OVA-challenged mice when compared with the control group. On the other hand, 3-MA-treated OVA group had a reduction in the pulmonary influx of cells located in the peribronchial and

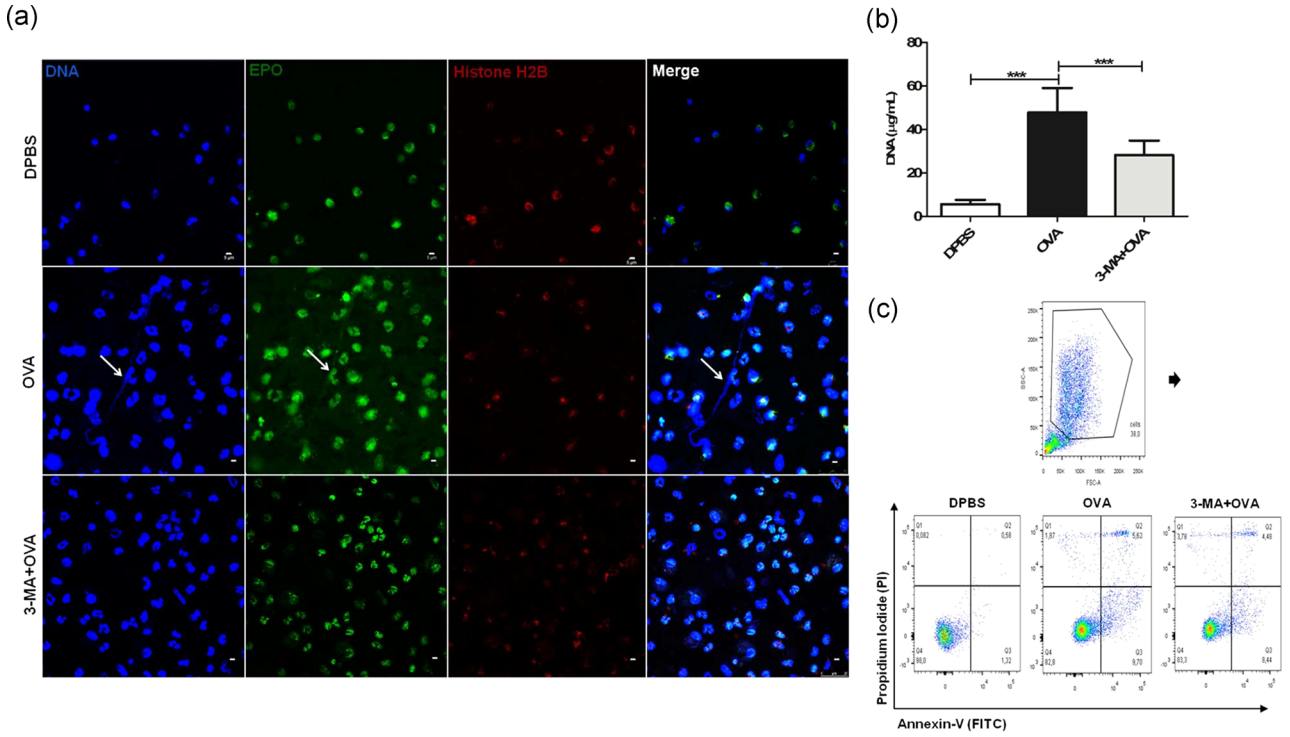

FIGURE 4 EETs release in the airway of OVA-challenged mice depends on autophagy without cell death. (a) Immunofluorescence microscopy of EETs in BALF eosinophils (×630 magnification, scale bars = 5 µm, arrows indicate EETs formation). BALF eosinophils incubated at 37°C with 5% carbon dioxide. Cells were fixed with 4% PFA and incubated with primary antibodies, anti-EPO, and anti-histone H2B. After this, cells were incubated with secondary antibodies, FITC anti-goat, followed by Hoechst 33342. Images were taken with a confocal microscope. (b) Quantification of extracellular DNA traps in BALF. Extracellular DNA quantification in BALF supernatants was performed with the Qubit dsDNA HS assay kit. (c) Analysis of cell death in BALF cells by Annexin-V/PI (Annexin-V (*x-axis*)/PI (*y-axis*). Cells were incubated with Annexin-V-FITC and PI and analyzed by flow cytometry. Data represent the mean ± *SD*, *n* = 10 animals per group. 3-MA: 3-methyladenine; ANOVA, analysis of variance; BALF, bronchoalveolar lavage fluid; DPBS, Dulbecco's phosphate buffered-saline; EETs, eosinophil extracellular traps; EPO, eosinophil peroxidase; FITC, fluorescein isothiocyanate; OVA, ovalbumin; PFA, paraformaldehyde; PI, propidium iodide; *SD*, standard deviation. ***$p < .001$ (one-way ANOVA followed by Tukey's test) [Color figure can be viewed at wileyonlinelibrary.com]

perivascular areas when compared with the OVA group (Figure 1h–j). In addition, OVA-challenge mice had an increase in goblet cells and mucus production compared with the control group. In contrast, 3-MA-treated OVA group had a reduction in goblet cells and mucus production compared with the OVA group (Figure 1k).

3.2 | 3-MA improves respiratory system mechanics

We evaluated whether the 3-MA treatment was capable of improving respiratory mechanics in an asthma model. Tissue damping and tissue elastance were significantly increased in the OVA-challenged mice compared with the DPBS group. In contrast, 3-MA treatment was able to reduce significantly tissue damping and tissue elastance compared with the OVA group. We did not observe differences between the groups in airway resistance (Figure 2a–c).

3.3 | 3-MA decreases inflammatory cytokines and NFκB p65 in lung

Later, we evaluated the effects of 3-MA treatment in inflammatory cytokines levels. We showed that OVA-challenged mice had an increase in IL-5, IL-13, IFN-Y, TNF-α, and IL-1β when compared with the control group. On the other hand, administration of 3-MA attenuated the levels of IL-5, IFN-Y, and IL-13 in the lung compared with the OVA group (Figure 2d–i). We did not observe differences between the groups in IL-10 levels. Due to the results found in inflammatory cytokines, NFκB p65 analysis was performed. Whereas OVA group had a significantly increased in NFκB p65 when compared with the control group, 3-MA treatment decreased NFκB p65 in the lung (Figure 2j).

3.4 | 3-MA decreases ROS production and increases CAT activity in lung

The effect of 3-MA on oxidative stress in OVA-challenged mice was evaluated. OVA group showed a significant increase in ROS production in the lung when compared with the control group. On the other hand, ROS formation in the 3-MA-treated OVA group showed a decrease when compared with the OVA group (Figure 3a). The effect of 3-MA in the enzymatic antioxidant defenses was also evaluated. OVA group promoted a significant decrease in CAT and GPx activities when compared with the control group (Figure 3c,d). 3-MA was able to increase CAT activity in the lung when compared with the OVA group

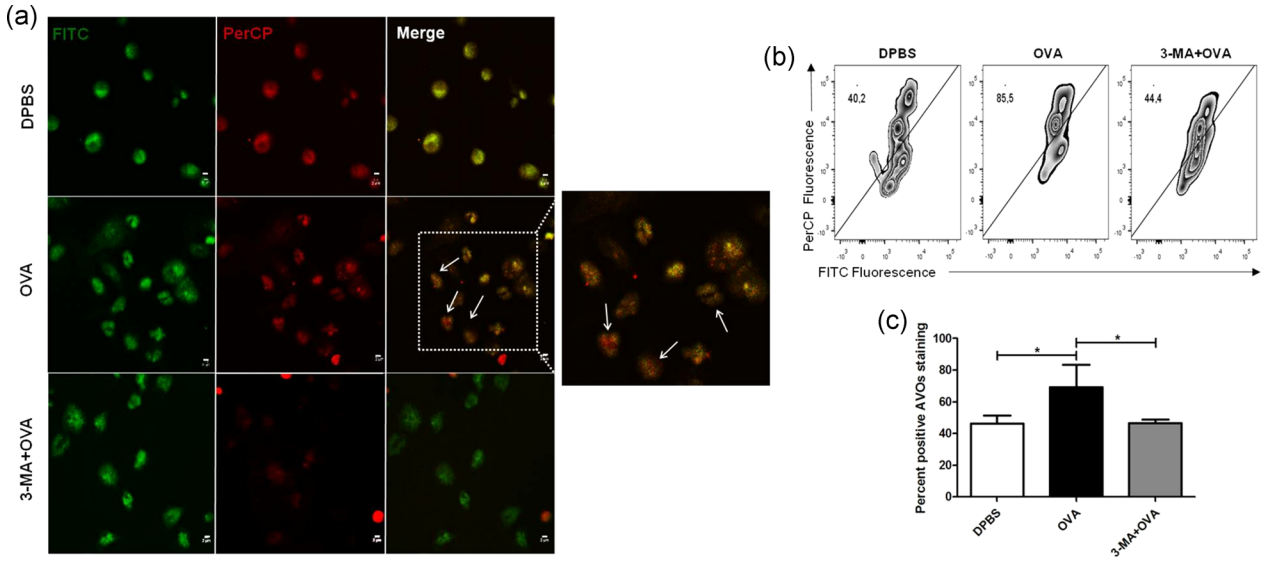

FIGURE 5 3-MA decreases AVOs formation in BALF eosinophils. (a) Detection and quantification of AVOs in BALF eosinophils. Analysis of AVOs in BALF eosinophils by immunofluorescence (×630 magnification, scale bars = 2 μm, FITC (Green) is showing cytoplasm and nucleus, PerCP (red) is showing AVOs). BALF eosinophils were plated and incubated at 37°C with 5% carbon dioxide. Cells were incubated with the AO dye at the final concentration of 1 μg/ml and visualized in a confocal microscope. (b,c) Quantification of AVOs in BALF eosinophils by flow cytometry (FITC [Green]) is showing cytoplasm and nucleus (*x-axis*)/ PerCP (Red) is showing AVOs (*y-axis*). BALF eosinophils were incubated with AO in the final concentration of 1 μg/ml and were analyzed by flow cytometry. Data represent the mean ± *SD*, *n* = 10 animals per group. 3-MA, 3-methyladenine; ANOVA, analysis of variance; AO, acridine orange; AVOs, acidic vesicle organelles; BALF, bronchoalveolar lavage fluid; DPBS, Dulbecco's phosphate buffered-saline; FITC, fluorescein isothiocyanate; OVA, ovalbumin; *SD*, standard deviation. *$p < .01$ (one-way ANOVA followed by Tukey's test) [Color figure can be viewed at wileyonlinelibrary.com]

(Figure 3c). We did not observe any significant difference in SOD activity between groups (Figure 3b). We also showed that the OVA group had a significant increase in SOD/CAT ratio when compared with the control group whereas 3-MA decreased this measure (Figure 3e).

3.5 | 3-MA improves mitochondrial energy metabolism and NA^+, K^+-ATPase activity in lung

We investigated the OVA effect in parameters of the mitochondrial energy metabolism (SDH, Complex II, and Complex IV) in the lung. About mitochondrial energy metabolism parameters, we observed that the OVA group had a significant decrease in SDH, Complex II, and Complex IV activities when compared with the control group, suggesting that OVA-challenged mice compromise electron transport chain function in the lung. We also investigated whether 3-MA treatment would be able to improve mitochondrial energy metabolism. Administration of 3-MA was able to increase significantly SDH and Complex II activity in the lung compared with the OVA group (Figure 3f–h). We decided to investigate also the 3-MA effect in NA^+, K^+-ATPase activity. We also showed that OVA group had a decrease in NA^+, K^+-ATPase when compared with the control group whereas 3-MA significantly increased its activity (Figure 3i).

3.6 | EETs release in the airway of OVA-challenged mice depend on autophagy without cell death

OVA-challenged mice had an increase in extracellular DNA concentrations in BALF when compared with the DPBS group. In immunofluorescence microscopy, we showed that eosinophils from asthmatic mice released EETs colocalized with EPO but did not colocalize with histone H2B (Figure 4a,b). We conducted an investigation to find out if 3-MA was able to reduce EETs formation in an asthma model. Autophagy inhibitor 3-MA decreased extracellular DNA concentrations in BALF from OVA-challenged mice. Similarly, in immunofluorescence microscopy we did not observe EETs formation in BALF eosinophils in 3-MA-treated OVA group, confirming our findings (Figure 4a,b). To discard the possibility of DNA extracellular found in BALF to be derived from dead cells, we performed flow cytometric analysis of Annexin-V and PI. EETs release was not due to cell death because cell viability remained high between the groups, showing that most cells present negative staining for Annexin-V and PI (Figure 4c). Altogether, these data suggest that EETs release in the airway of OVA-challenged mice depend on autophagy without cell death.

3.7 | 3-MA decreases AVOs formation and LC3B immunocontent in airway

We stained BALF cells with AO dye to evaluate AVOs formation. We showed that OVA-challenged mice had an increase in AVOs formation in BALF eosinophils stained with AO and evaluated by immunofluorescence. In addition, 3-MA was able to reduce AVOs in BALF eosinophils when compared with the OVA group (Figure 5a). Similarly, in cytometry analysis, we observed that in OVA-challenged mice there was an increase in AVOs whereas 3-MA decreased AVOs formation in BALF cells (Figure 5b,c). To confirm that 3-MA decreased autophagy in

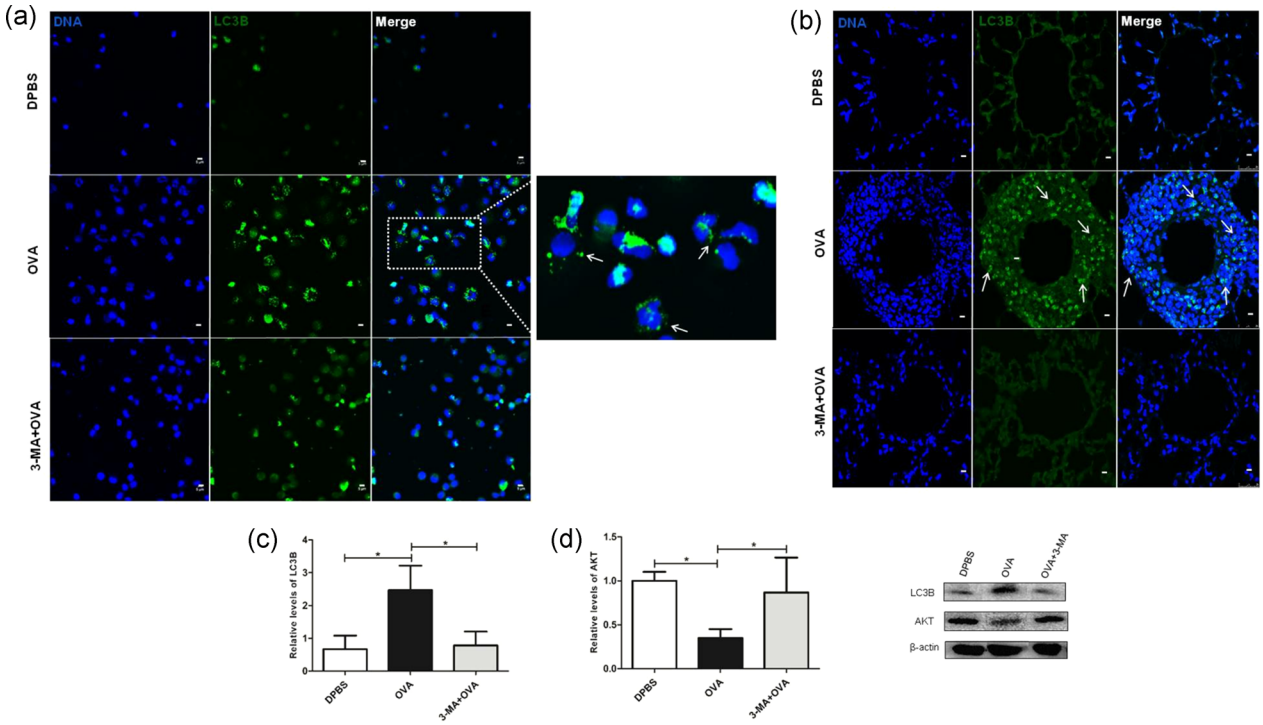

FIGURE 6 3-MA decreases LC3B and AKT immunocontents in the airway. (a,b) Analysis of LC3B in BALF eosinophils and lung tissue by immunofluorescence (630x magnification, scale bars = 5 μm). BALF eosinophils or lung sections were incubated with anti-LC3B, followed by incubation with secondary antibody, FITC anti-rabbit. Cells were stained with Hoechst 33342 and visualized by confocal microscopy. (b,c) Analysis of LC3B and AKT in the lung by Western blot. Lung tissues were homogenized and analyzed by Western blot for the immunocontent of LC3B and AKT. The LC3B and AKT were standardized with respect to actin levels and all was expressed as a percentage of controls (DPBS group). Data represent the mean ± *SD*, *n* = 10 animals per group. 3-MA, 3-methyladenine; ANOVA, analysis of variance; AKT: protein kinase B, BALF, bronchoalveolar lavage fluid; DPBS, Dulbecco's phosphate buffered-saline; FITC, fluorescein isothiocyanate; LC3B, light chain 3B; OVA, ovalbumin; *SD*, standard deviation. *$p < .01$ (one-way ANOVA followed by Tukey's test) [Color figure can be viewed atwileyonlinelibrary.com]

the asthma model, we analyzed LC3B protein in lung tissue and in BALF eosinophils. LC3B protein is an indicator of autophagosome formation and is widely analyzed to detect autophagic activity. We showed that in OVA-challenged mice there was an increase in LC3B in BALF eosinophils and lung tissue evaluated by immunofluorescence and western blot. In contrast, we showed that autophagy inhibitor 3-MA was able to reduce LC3B in BALF eosinophils and lung tissue when compared with the OVA group (Figure 6a–c).

3.8 | 3-MA decreases AKT immunocontent in lung

Finally, the effect of 3-MA treatment in AKT immunocontent was investigated. AKT protein is widely studied in the regulation of autophagy (Ellington, Berhow, & Singletary, 2006). We demonstrated that the OVA group had a significant decrease in AKT immunocontent in the lung when compared with the control group. In contrast, 3-MA-treated OVA group had an increase in AKT when compared with the OVA group (Figure 6d).

4 | DISCUSSION

Asthma is characterized by the enhancement in inflammatory cells in the lung such as eosinophil (Lambrecht & Hammad, 2015). Although there is an enhancement in DNA extracellular traps formation by eosinophils, mechanism of EETs release and their pathophysiologic role in asthma are poorly understood (Cunha et al., 2014; Dworski et al., 2011). Moreover, evidence has been observed the participation of autophagy in asthma immunopathology (Liu et al., 2016; Poon et al., 2012). In our study, we showed the first evidence that autophagy is needed for EETs formation in the airway in asthmatic mice. We demonstrated that autophagy inhibition significantly improves airway inflammation, respiratory system mechanics, oxidative stress, mitochondrial energy metabolism, Na^+, K^+-ATPase activity, and reduces EETs release.

Studies have reported an increase in autophagosomes formation in the airway in asthma (Jiang et al., 2017; Liu et al., 2016). Evidence also suggests a relation between genetic polymorphisms of ATG5 and lung remodeling and impairment in respiratory system mechanics in asthma (Martin et al., 2012; Poon et al., 2012). Ban et al. (2015) observed an increase in autophagy in sputum granulocytes of asthmatic patients. Poon et al. (2012) reported an increase of autophagosome in fibroblasts and epithelium of asthmatic patients. Autophagy plays a critical role in differentiation, survival, and chemotaxis of cells (Conway et al., 2013). In our study, to investigate the role of autophagy in asthma, an experimental asthma model was developed. We showed that in the OVA group there was an increase

in inflammatory cells, goblet cells hyperplasia, EPO activity, and a decrease in respiratory system mechanics, which are typical pathologic features of asthma. In this model, there is a significant high influx of eosinophils in the airway. We reported that autophagy inhibition with 3-MA decreased total cell counts as well as eosinophils and neutrophils counts in BALF when compared with the OVA group. Furthermore, we showed that the 3-MA-treated OVA group had a reduction in the pulmonary influx of cells when compared with the OVA group. Our results are corroborated by studies, which show that autophagy inhibition decreases inflammatory cells especially the eosinophils in the airway in asthma models (Liu et al., 2016, Jiang et al., 2017). We showed that in OVA group there was an increase in eosinophil migration into airway and 3-MA was able to decrease lung eosinophilia. So, we decided to evaluate EPO activity in BALF, which is a cytotoxic granular protein of the eosinophils (Sanz et al., 1997). In EPO granular protein analysis, OVA increased the EPO activity in BALF whereas the 3-MA treatment decreased significantly EPO activity. In this context, Ban et al. (2015) showed that autophagy inhibition decreased the expression of eosinophil cationic protein in human eosinophil-like cells stimulated with IL-5. After that, we demonstrated that in the 3-MA-treated OVA group there was a reduction in goblet cells and mucus compared with the OVA group. In agreement to our result, evidence has shown that autophagy inhibition decreases goblet cells and mucus in the airway from the asthma model (Jiang et al., 2017; Liu et al., 2016). Poon et al. (2012) reported a relation between impairment in respiratory system mechanics in asthma and ATG polymorphism. To assess whether autophagy has an effect in respiratory system mechanics in asthmatic mice, we evaluated airway resistance, tissue damping, and tissue elastance. We showed that 3-MA was able to reduce tissue damping and tissue elastance but did not alter airway resistance when compared with the OVA group. In accordance with our results, Liu et al. (2016) observed an improvement in respiratory system mechanics in an ATG5 knockdown murine asthma model. This result probably occurred because of a decrease in mucus and lung inflammation. Thus, 3-MA treatment can be an important alternative to decrease inflammatory cells, goblet cells hyperplasia, and improve respiratory system mechanics in asthma via suppression of autophagy.

Inflammatory cytokines play an essential role in lung remodeling, mucus hypersecretion, and inflammation in asthma (Barnes, 2008). Recently, autophagy function has been widely investigated in adaptive and innate immunity, more specifically in Th2 immune response. Furthermore, autophagy is crucial for lymphocyte differentiation and survival (Puleston & Simon, 2014). We observed that in OVA-challenged mice there was an increase in IL-5, IL-13, IFN-Y, TNF-α, and IL-1β in the lung. In contrast, autophagy inhibition with 3-MA attenuated the level of IL-5, IFN-Y, and IL-13. In this context, evidence has reported that IL-5, IFN-Y, and IL-13 cytokines enhance autophagy (Ban et al., 2015; Jyothula & Eissa, 2013). In agreement to our results, evidence has reported that autophagy inhibition decreases inflammatory cytokines in the lung (Jiang et al., 2017; Liu et al., 2016). Moreover, autophagy plays a crucial role in the phosphorylation of NFκB (Criollo et al., 2012). When NFκB is phosphorylated, p65 and p50 subunits go to the nucleus and promote the production of inflammatory cytokines (Oka, Kamata, Kamata, Yagisawa, & Hirata, 2000). We hypothesized that autophagy inhibition could reduce inflammatory cytokines in the lung via NFκB p65 inhibition. We reported that in the OVA-challenged mice there was an increase in NFκB p65 whereas the 3-MA treatment decreased NFκB p65 in the lung. We suggested that in asthma 3-MA treatment can decrease NFκB p65 and, consequently, reduce inflammatory cytokines in the lung.

Evidence has reported that an imbalance between the ROS formation and antioxidant defense mechanisms contribute to asthma immunopathology (Andreadis, Hazen, Comhair, & Erzurum, 2003; Cunha et al., 2016). Moreover, mitochondrial ROS is the main trigger for autophagy induction (Filomeni, Zio, & Cecconi, 2015). In contrast, antioxidant defenses serve as natural down regulators of autophagy (Scherz-Shouval & Elazar, 2011). We evaluated whether autophagy inhibition affects oxidative stress in OVA-challenged mice. In the OVA-challenged mice, there was an increase in ROS formation in the lung. We verified that in the OVA group there was a decrease in CAT and GPx activities, but there was not an alteration in SOD, suggesting an unbalance in oxidant-antioxidant status. SOD promotes the dismutation of superoxide, and CAT and GPx induce the reduction of hydrogen peroxide (Cunha et al, 2011). We suggested that an increase in ROS formation did not increase the consumption of the SOD that induces the dismutation of superoxide in hydrogen peroxide. However, normal levels of SOD increase hydrogen peroxide formation whereas insufficient CAT and GPx activities enhance hydrogen peroxide accumulation, increasing oxidative stress in airway. In addition, ROS formation in the 3-MA-treated OVA group had a decrease when compared with the OVA group. In this context, Dickinson et al. (2018) showed that autophagy was needed for the intracellular superoxide production in airway epithelial cells. Furthermore, we showed that 3-MA was able to increase CAT activity in the lung. AKT pathway can be signalized by oxidative stress (Song et al., 2008). AKT is altered in inflammatory diseases and regulates many cellular processes including survival, proliferation, growth, metabolism, angiogenesis, and oxidative stress, which are also important in asthma (Song et al., 2008; Zou, Ding, Niu, Fu, & Liu, 2018). Studies on asthma pathogenesis indicate that AKT modulates AHR, inflammation, and vascular permeability (Jiang et al., 2017; Kim et al., 2010; Lee et al., 2006; Wang et al., 2014). We observed that in the OVA group there was a decrease in AKT immunocontent whereas the opposite outcome was reported in the 3-MA-treated OVA group. Corroborating our results, Zou et al. (2018) demonstrated a decrease in AKT levels in asthmatic mice. Nuclear factor erythroid 2-related factor 2 (Nrf2) may be activated by the AKT (Ma, 2013). Antioxidant response element is activated by the Nrf2 in the nucleus and consequently increases the generation of antioxidant enzymes (Ma, 2013). Therefore, we reported that autophagy inhibition with 3-MA decreases oxidative stress in asthmatic mice.

Exposition of cells to ROS may increase oxidative injury to the mitochondria, which may inactivate the electron transport chain

(Reddy, 2006). In this context, evidence has shown a relation between inflammatory lung diseases and mitochondrial dysfunction (Aguilera-Aguirre et al., 2009; M. J. Cunha et al., 2014). We verified that in the OVA-challenged mice there was a reduction in Complex II, SDH, and Complex IV, suggesting that in OVA-challenged mice there is damage in the electron transport chain. Aguilera-Aguirre et al. (2009) verified that alteration of the mitochondrial energy metabolism function increases inflammation in the lung in allergic patients. Moreover, Mabalirajan et al. (2008) reported a reduction in ATP synthesis and in Complex IV activity in the airway in OVA-challenged mice. We observed that autophagy inhibition with 3-MA was able to increase Complex II and SDH activity in the lung. We suggested that 3-MA decreased the damage in the electron transport chain due to a decrease in oxidative stress in lung, and consequently, improved mitochondrial energy metabolism.

Na^+, K^+-ATPase controls cellular ionic gradient and its function is vulnerable to ROS formation and to ATP depletion (Schweinberger et al., 2014). Reduction in Na^+, K^+-ATPase activity alters electrical membrane potential, downregulates the responses to β-agonists in β-adrenergic receptors, increases bronchoconstriction, and activation of leukocytes (Agrawal et al., 2005). Due to damage of the electron transport chain and ATP reduction, we verified that in the OVA-challenged mice there was a reduction in the NA^+, K^+-ATPase. The synthesis of ATP in mitochondrial is performed mainly on the respiratory chain Complexes I–IV (Bratic & Trifunovic, 2010). However, injury to the electron transport chain may decrease ATP production (Schulz et al., 2012; Wen & Garg, 2010). We believe that excessive ROS production may have also contributed to the reduction of NA^+, K^+-ATPase enzyme activity in the lung. Increase in ROS can oxidize the Na^+, K^+-ATPase protein and decrease its activity (Srikanthan, Shapiro, & Sodhi, 2016). In accordance with our result, Agrawal et al. (2005) reported a reduction in Na^+, K^+-ATPase activity in leukocytes in asthmatic patients. We also reported that 3-MA treatment significantly increased the NA^+, K^+-ATPase activity in the lung. We suggested that autophagy inhibition with 3-MA increased Na^+, K^+-ATPase activity due to the improvement of mitochondrial energy metabolism, and consequently, restored ATP levels. Moreover, a decrease in ROS in the 3-MA-treated OVA group reduced Na^+, K^+-ATPase damage, and, consequently, increased Na^+, K^+-ATPase activity in the airway.

Studies have shown an increase in EETs formation in the airway in asthma (Cunha et al., 2014; Dworski et al., 2011). EETs formation may increase airway damage and mucus viscosity, and consequently, decrease respiratory system mechanics. We showed that OVA-challenged mice presented an increase in extracellular DNA levels. Moreover, in immunofluorescence microscopy, we observed that eosinophils from asthmatic mice released EETs colocalized with EPO. We demonstrated that EETs were not colocalized with histone HB2, which suggests that the DNA formed by EETs is of mitochondrial origin. Histones compact and protect nuclear DNA; however, in mitochondrial DNA there are no histones (Alexeyev et al, 2013). Afterward, we investigated whether autophagy would be necessary for EETs formation in the lung in OVA-challenged mice. Administration of autophagy inhibitor, 3-MA, decreased extracellular DNA concentrations in BALF from OVA-challenged mice. Similarly, in immunofluorescence microscopy, we did not verify EETs formation in BALF eosinophils in the 3-MA-treated OVA group, which corroborates our findings. Altogether, these results indicate that autophagy is indispensable for EETs formation in the airway in OVA-challenged mice. Thus, inhibition autophagy with 3-MA may reduce airway immunopathology in asthma through the decrease in EETs release. Some evidence has reported that EETs release is due to eosinophil death; others have reported that they can remain viable (Cunha et al., 2016; Ueki et al., 2016; Yousefi et al., 2008). We verified that EETs formation was not due to cell death once we have demonstrated that BALF cell viability remained high in control, asthmatic, and treated mice groups. Thus, we demonstrated that EETs release in asthma is dependent on autophagy in an active process without cell death.

Autophagy induces the cytoplasmic sequestration of proteins from the lytic component and it is defined by the formation of AVOs, such as autolysosomes (Anderson, Falck, Goldstein, & Brown, 1984). We verified that the OVA group had an increase in AVOs in BALF eosinophils while that autophagy inhibition with 3-MA was able to reduce AVOs when compared with the OVA group. Evidence has shown an enhancement in autophagosomes number in cells from asthmatic patients and in experimental asthma models (Liu et al., 2016; Pham et al., 2016). A characteristic feature of autophagy is the presence of autophagosomes. LC3 is a protein needed for autophagosome formation and is an indicator of autophagosome (Cheng et al., 2017). Ban et al. (2015) observed an increase in immunocontent of LC3-II in sputum granulocytes from patients with severe asthma. Similarly, we showed that LC3B immunocontent was higher in BALF eosinophils and lung tissue in the OVA group when compared with the control group. 3-MA treatment decreased LC3B in BALF eosinophils and lung tissue when compared with the OVA group. AKT protein is extensively analyzed in the control of autophagy (Ellington et al., 2006). We demonstrated that in the OVA-challenged mice there was a reduction in AKT immunocontent in lung whereas 3-MA-treated OVA group increased AKT immunocontent when compared with the OVA group. In this context, AKT actives mTOR, and consequently, suppresses autophagy (Degtyarev et al., 2008). AKT phosphorylation inactive Forkhead box O3, which regulates autophagy-related genes such as LC3 and Bnip3 (Mammucari et al., 2007). In contrast, PTEN inhibits AKT and positively regulates autophagy (Arico et al., 2001). Altogether, our results report that 3-MA treatment was able to reduce autophagy in BALF eosinophils and lung in OVA-challenged mice.

In summary, this is the first study to show that viable eosinophils release EETs dependent on autophagy in the airway of an experimental asthma model. Autophagy inhibition with 3-MA improved airway inflammation, respiratory system mechanics, oxidative stress, mitochondrial energy metabolism, Na^+, K^+-ATPase activity, and also reduced EETs formation in lung from asthmatic mice. Therefore, we could show that modulation of eosinophils

autophagy regulates the activation process of EETs release in asthma.

ACKNOWLEDGMENTS

We thank Rodrigo Godinho de Souza, Betânia Souza Freitas, and Krist Helen Antunes Fernandes for their technical assistance. This study was financed in part by the Coordenação de Aperfeiçoamento de Pessoal de Nível Superior (CAPES) and Conselho Nacional de Desenvolvimento Científico e Tecnológico (CNPq), Brazil.

CONFLICT OF INTERESTS

The authors declare that there is no conflict of interests.

AUTHOR CONTRIBUTIONS

J. S. S. and A. A. C. designed the studies. J. S. S., A. A. C., G. L. A., D. B. K., M. S., E. P. M., F. F., F. S., R. B. G., and R. V. B. contributed to the data collection. J. S. S., A. A. C., P. M. P., and A. T. S. W. analyzed and interpreted the work. J. S. S. and A. A. C. wrote the manuscript. All authors have read, revised and approved the final version of this manuscript.

ORCID

Aline Andrea da Cunha http://orcid.org/0000-0002-1059-360X

REFERENCES

Aebi, H. (1984). Catalase, in vitro. *Methods Enzymology*, *105*, 121–126. https://doi.org/10.1016/S0076-6879(84)05016-3

Agrawal, A., Agrawal, K. P., Ram, A., Sondhi, A., Chhabra, S. K., Gangal, S. V., & Dolly, M. (2005). Basis of rise in intracellular sodium in airway hyperresponsiveness and asthma. *Lung*, *183*, 375–387. https://doi.org/10.1007/s00408-005-2549-0

Aguilera-Aguirre, L., Bacsi, A., Saavedra-Molina, A., Kurosky, A., Sur, S., & Boldogh, I. (2009). Mitochondrial dysfunction increases allergic airway inflammation. *Journal Immunology*, *183*, 5379–5387. https://doi.org/10.4049/jimmunol.0900228

Alexeyev, M., Shokolenko, I., Wilson, G., & LeDoux, S. (2013). The maintenance of mitochondrial DNA integrity-critical analysis and update. The unfolded protein response in lung disease. *Proceedings of the American Thoracic Society*, *7*, 356–362. https://doi.org/10.1101/cshperspect.a012641.

Anderson, R. G., Falck, J. R., Goldstein, J. L., & Brown, M. S. (1984). Visualization of acidic organelles in intact cells by electron microscopy. *Proceedings of the National Academy of Sciences of the United States of America*, *81*, 4838–4842.

Andreadis, A. A., Hazen, S. L., Comhair, S. A., & Erzurum, S. C. (2003). Oxidative and nitrosative events in asthma. *Free Radical Biology and Medicine*, *35*, 213–225. https://doi.org/10.1016/S0891-5849(03)00278-8

Arico, S., Petiot, A., Bauvy, C., Dubbelhuis, P. F., Meijer, A. J., Codogno, P., & Ogier-Denis, E. (2001). The tumor suppressor PTEN positively regulates macroautophagy by inhibiting the phosphatidylinositol 3-kinase/protein kinase B pathway. *Journal of Biological Chemistry*, *276*, 35243–35246. https://doi.org/10.1074/jbc.C100319200

Ban, G. Y., Pham, D. L., Trinh, H. K., Lee, S. I., Suh, D. H., Yang, E. M., & Park, H. S. (2015). Autophagy mechanisms in sputum and peripheral blood cells of patients with severe asthma: A new therapeutic target. *Clinical and Experimental Allergy*, *46*, 48–59. https://doi.org/10.1111/cea.12585

Barnes, P. J. (2008). The cytokine network in asthma and chronic obstructive pulmonary disease. *The Journal of Clinical Investigation*, *118*, 3546–3456. https://doi.org/10.1172/JCI36130

Bradford, M. M. (1976). A rapid and sensitive method for the quantitation of microgram quantities of protein utilizing the principle of protein-dye binding. *Analytical Biochemistry*, *72*, 248–254. https://doi.org/10.1016/0003-2697(76)90527-3

Bratic, I., & Trifunovic, A. (2010). Mitochondrial energy metabolism and ageing. *Biochimica et Biophysica Acta (BBA) – Bioenergetics*, *1797*, 961–967. https://doi.org/10.1016/j.bbabio.2010.01.004

Cheng, Z., Wang, X., Dai, L., Jia, L., Jing, X., & Liu, Y.et al. (2017). Suppression of microRNA-384 enhances autophagy of airway smooth muscle cells in asthmatic mouse. *8*, 67933–67941.

Comhair, S. A., & Erzurum, S. C. (2010). Redox control of asthma: Molecular mechanisms and therapeutic opportunities. *Antioxidants & Redox Signaling*, *12*, 93–124. https://doi.org/10.1089/ars.2008.2425

Conway, K. L., Kuballa, P., Khor, B., Zhang, M., Shi, H. N., Virgin, H. W., & Xavier, R. J. (2013). ATG5 regulates plasma cell differentiation. *Autophagy*, *9*, 528–537. https://doi.org/10.4161/auto.23484

Criollo, A., Chereau, F., Malik, S. A., Niso-Santano, M., Mariño, G., Galluzzi, L., & Kroemer, G. (2012). Autophagy is required for the activation of NFκB. *Cell Cycle*, *11*, 194–199. https://doi.org/10.4161/cc.11.1.18669

Cunha, A. A., Nuñez, N. K., Souza, R. G., Vargas, H. M. V., Silveira, J. S., Antunes, G. L., … Pitrez, P. M. (2016). Recombinant human deoxyribonuclease therapy improves airway resistance and reduces DNA extracellular traps in a murine acute asthma model. *Experimental Lung Research*, *42*, 66–74. https://doi.org/10.3109/01902148.2016.1143537

Cunha, A. A., Porto, B. N., Nuñez, N. K., Souza, R. G., Vargas, M. H., Silveira, J. S., … Pitrez, P. M. (2014). Extracellular DNA traps in bronchoalveolar fluid from a murine eosinophilic pulmonary response. *Allergy*, *69*, 1696–1700. https://doi.org/10.1111/all.12507

Cunha, M. J., Cunha, A. A., Scherer, E. B., Machado, F. R., Loureiro, S. O., & Jaenisch, R. B. (2014). Experimental lung injury promotes alterations in energy metabolism and respiratory mechanics in the lungs of rats: Prevention by exercise. *Molecular Cell Biochemical*, *389*, 229–238. https://doi.org/10.1007/s11010-013-1944-8.

Cunha, A. A., Ferreira, A. G. K., da Cunha, M. J., Pederzolli, C. D., Becker, D. L., & Coelho, J. G. (2011). Chronic hyperhomocysteinemia induces oxidative damage in the rat lung. *Molecular and Cellular Biochemistry*, *358*, 153–160. https://doi.org/10.1007/s11010-011-0930-2.

Degtyarev, M., DeMazière, A., Orr, C., Lin, J., Lee, B. B., Tien, J. Y., … Lin, K. (2008). Akt inhibition promotes autophagy and sensitizes PTEN-null tumors to lysosomotropic agents. *Journal Cell Biology*, *183*, 101–116. https://doi.org/10.1083/jcb.200801099

Dworski, R., Simon, H. U., Hoskins, A., & Yousefi, S. (2011). Eosinophil and neutrophil extracellular DNA traps in human allergic asthmatic airways. *Journal Allergy Clinical Immunology*, *127*, 1260–1266. https://doi.org/10.1016/j.jaci.2010.12.1103

Ellington, A. A., Berhow, M. A., & Singletary, K. W. (2006). Inhibition of Akt signaling and enhanced ERK1/2 activity are involved in induction of macroautophagy by triterpenoid B-group soyasaponins in colon cancer cells. *Carcinogenesis*, *27*, 298–306. https://doi.org/10.1093/carcin/bgi214

Filomeni, G., Zio, D. D., & Cecconi, F. (2015). Oxidative stress and autophagy: The clash between damage and metabolic needs. *Cell Death & Differentiation*, *22*, 377–388. https://doi.org/10.1038/cdd.2014.150

Fischer, J. C., Ruitenbeek, W., Berden, J. A., Trijbels, J. M. F., Veerkamp, J. H., Stadhouders, A. M., … Janssen, A. J. (1985). Differential investigation of the capacity of succinate oxidation in human skeletal muscle. *Clinical Chemical Acta*, *153*, 23–36. https://doi.org/10.1016/0009-8981(85)90135-4

Hantos, Z., Daróczy, B., Suki, B., Nagy, S., & Fredberg, J. J. (1992). Input impedance and peripheral inhomogeneity of dog lungs. *Journal of Applied Physiology*, *72*, 168–178. https://doi.org/10.1152/jappl.1992.72.1.168

Jiang, X., Fang, L., Wu, H., Mei, X., He, F., Ding, P., & Liu, R. (2017). TLR2 Regulates allergic airway inflammation and autophagy through PI3K/Akt signaling pathway. *Inflammation*, *40*, 1382–1392. https://doi.org/10.1007/s10753-017-0581-x

Jyothula, S. S., & Eissa, N. T. (2013). Autophagy and role in asthma. *Current Opinion in Pulmonary Medicine*, *19*, 30–35. https://doi.org/10.1097/MCP.0b013e32835b1150

Kenno, S., Perito, S., Mosci, P., Vecchiarelli, A., & Monari, C. (2016). Autophagy and Reactive oxygen species are involved in neutrophil extracellular traps release induced by *C. albicans* morphotypes. *Frontier Microbiology*, *8*, 879–893. https://doi.org/10.3389/fmicb.2016.00879

Kim, S. R., Lee, K. S., Park, H. S., Park, S. J., Min, K. H., Moon, H., … Lee, Y. C. (2010). HIF1a inhibition ameliorates an allergic airway disease via VEGF suppression in bronchial epithelium. *European Journal of Immunology*, *40*, 2858–2869. https://doi.org/10.1002/eji.200939948

Lambrecht, B. N., & Hammad, H. (2015). The immunology of asthma. *Nature Immunology*, *16*, 45–56. https://doi.org/10.1038/ni.3049

LeBel, C. P., Ischiropoulos, H., & Bondy, S. C. (1992). Evaluation of the probe 2′,7′-dichlorofluorescin as an indicator of reactive oxygen species formation and oxidative stress. *Chemical Research Toxicology*, *5*, 227–231. https://doi.org/10.1021/tx00026a012

Lee, K. S., Park, S. J., Kim, S. R., Min, K. H., Jin, S. M., Puri, K. D., & Lee, Y. C. (2006). Phosphoinositide 3-kinase-delta inhibitor reduces vascular permeability in a murine model of asthma. *Journal of Allergy and Clinical Immunology*, *118*, 403–409. https://doi.org/10.1016/j.jaci.2006.04.041.

Liu, J. N., Suh, D. H., Trinh, H. K., Chwae, Y. J., Park, H. S., & Shin, Y. S. (2016). The role of autophagy in allergic inflammation: A new target for severe asthma. *Experimental Molecular Medicine*, *48*, e243. https://doi.org/10.1038/emm.2016.38

Lowry, O. H., Rosebrough, N. J., Farr, A. L., & Randall, R. J. (1951). Protein measurement with the Folin phenol reagent. *Journal of Biological Chemistry*, *193*, 265–275.

Ma, Q. (2013). Role of Nrf2 in oxidative stress and toxicity. *Annual Review of Pharmacology and Toxicology*, *53*, 401–426. https://doi.org/10.1146/annurev-pharmtox-011112-140320

Mabalirajan, U., Dinda, A. K., Kumar, S., Roshan, R., Gupta, P., Sharma, S. K., & Ghosh, B. (2008). Mitochondrial structural changes and dysfunction are associated with experimental allergic asthma. *Journal Immunology*, *181*, 3540–3548. https://doi.org/10.4049/jimmunol.181.5.3540

Mammucari, C., Milan, G., Romanello, V., Masiero, E., Rudolf, R., Del Piccolo, P., … Sandri, M. (2007). FoxO3 controls autophagy in skeletal muscle in vivo. *Cell Metabolism*, *6*, 458–471. https://doi.org/10.1016/j.cmet.2007.11.001

Marklund, S., L. (1985). Pyrogallol auto oxidation. In R. A. Greenwald (Ed.), *Handbook for oxygen radical research*. Boca Raton, Florida: CRC Press.

Martin, L. J., Gupta, J., Jyothula, S. S., Butsch, K. M., Biagini, M. J. M., Patterson, T. L., … Hershey, G. K. (2012). Functional variant in the autophagy-related 5 gene promotor is associated with childhood asthma. *PLoS One*, *7*, e33454. https://doi.org/10.1371/journal.pone.0033454

Mizushima, N. (2007). Autophagy: Process and function. *Genes & Development*, *21*, 2861–2873. https://doi.org/10.1101/gad.1599207

Oka, S., Kamata, H., Kamata, K., Yagisawa, H., & Hirata, H. (2000). N-acetylcysteine suppresses TNF-induced NF-kappaB activation through inhibition of IkappaB kinases. *Federation of European Biochemical Societies Letter*, *472*, 196–202. https://doi.org/10.1016/S0014-5793(00)01464-2

Pham, D. L., Ban, G. Y., Kim, S. H., Shin, Y. S., Ye, Y. M., Chwae, Y. J., & Park, H. S. (2017). Neutrophil autophagy and extracellular DNA traps contribute to airway inflammation in severe asthma. *Clinical Experimental Allergy*, *47*, 57–70. https://doi.org/10.1111/cea.12859

Pham, D. L. , Kim, S. H. , Losol, P. , Yang, E. M. , Shin, Y. S. , Ye, Y. M. , et al. Association of autophagy related gene polymorphisms with neutrophilic airway inflammation in adult asthma. *The Korean Journal of Internal Medicine* 2016;*31*, 375-385 https://doi.org/10.3904/kjim.2014.390

Poon, A., Eidelman, D., Laprise, C., & Hamid., Q. (2012). ATG5, autophagy and lung function in asthma. *Autophagy*, *8*, 694–695. https://doi.org/10.4161/auto.19315

Puleston, D. J., & Simon, A. K. (2014). Autophagy in the immune system. *Immunology*, *141*, 1–8. https://doi.org/10.1111/imm.12165

Reddy, P. H. (2006). Mitochondrial oxidative damage in aging and Alzheimer's disease: Implications for mitochondrially targeted antioxidant therapeutics. *Journal of Biomedicine and Biotechnology*, *3*, 1–13. https://doi.org/10.1155/JBB/2006/31372

Remijsen, Q., Vanden, B. T., Wirawan, E., Asselbergh, B., Parthoens, E., DeRycke, R., … Vandenabeele, P. (2011). Neutrophil extracellular trap cell death requires both autophagy and superoxide generation. *Cell Research*, *21*, 290–304. https://doi.org/10.1038/cr.2010.150

Rueden, C. T., Schindelin, J., Hiner, M. C., DeZonia, B. E., Walter, A. E., Arena, E. T., & Eliceiri, K. W. (2017). ImageJ2: ImageJ for the next generation of scientific image data. *BMC Bioinformatics*, *18*, 529. https://doi.org/10.1186/s12859-017-1934-z

Rustin, P., Chretien, D., Bourgeron, T., Gérard, B., Rötig, A., Saudubray, J. M., & Munnich, A. (1994). Biochemical and molecular investigations in respiratory chain deficiencies. *Clinical Chemical Acta*, *228*, 35–51. https://doi.org/10.1016/0009-8981(94)90055-8

Sanz, M. L., Parra, A., Prieto, I., Dieguez, I., & Oehling, A. K. (1997). Serum eosinophil peroxidase (EPO) levels in asthmatic patients. *Allergy*, *52*, 417–422. https://doi.org/10.1111/j.1398-9995.1997.tb01021.x

Scherz-Shouval, R., & Elazar, Z. (2011). Regulation of autophagy by ROS: Physiology and pathology. *Trends Biochemical Sciences*, *36*, 30–38. https://doi.org/10.1016/j.tibs.2010.07.007

Schulz, K. L., Eckert, A., Rhein, V., Mai, S., Haase, W., Reichert, A. S., … Leuner, K. (2012). A new link to mitochondrial impairment in tauopathies. *Molecular Neurobiology*, *46*, 205–216. https://doi.org/10.1007/s12035-012-8308-3

Schweinberger, B. M., Schwieder, L., Scherer, E., Sitta, A., Vargas, C. R., & Wyse, A. T. S. (2014). Development of an animal model fore gestational hypermethioninemia in rat and its effect on brain Na^+, K^+-ATPase/$Mg2^+$-ATPase activity and oxidative status of the offspring. *Metabolic Brain Disease*, *29*, 153–160. https://doi.org/10.1007/s11011-013-9451-x

Simon, D., Hoesli, S., Roth, N., Staedler, S., Yousefi, S., & Simon, H. U. (2011). Eosinophil extracellular DNA traps in skin diseases. *Journal Allergy Clinical Immunology*, *127*, 194–199. https://doi.org/10.1016/j.jaci.2010.11.002

Song, Y. S., Narasimhan, P., Kim, G. S., Jung, J. E., Park, E.-H., & Chan, P. H. (2008). The role of Akt signaling in oxidative stress mediates NF-κB activation in mild transient focal cerebral ischemia. *Journal of Cerebral Blood Flow and Metabolism*, *28*, 1917–1926. https://doi.org/10.1038/jcbfm.2008.80

Srikanthan, K., Shapiro, J. I., & Sodhi, K. (2016). The role of Na/K-ATPase signaling in oxidative stress related to obesity and cardiovascular disease. *Molecules*, *21*, E1172. https://doi.org/10.3390/molecules21091172

Strath, M., Warren, D. J., & Sanderson, C. J. (1985). Detection of eosinophils using an eosinophil peroxidase assay. Its use as an assay for eosinophil differentiation factors. *Journal Immunology Methods*, *83*, 209–215. https://doi.org/10.1016/0022-1759(85)90242-X

Ueki, S., Konno, Y., Takeda, M., Moritoki, Y., Hirokawa, M., Matsuwaki, Y., … Weller, P. F. (2016). Eosinophil extracellular trap cell death-derived DNA traps: Their presence in secretions and functional attributes. *The Journal of Allergy and Clinical Immunology*, *137*, 258–267. https://doi.org/10.1016/j.jaci.2015.04.041

Wang, J., Li, F., Yang, M., Wu, J., Zhao, J., Gong, W., … Dong, L. (2014). FIZZ1 promotes airway remodeling through the PI3K/Akt signaling pathway in asthma. *Experimental and Therapeutic Medicine*, *7*, 1265–1270. https://doi.org/10.3892/etm.2014.1580

Wen, J. J., & Garg, N. J. (2010). Mitochondrial complex III defects contribute to inefficient respiration and ATP synthesis in the myocardium of Trypanosoma cruzi-infected mice. *Antioxidants & Redox Signaling*, *12*, 27–37. https://doi.org/10.1089/ARS.2008.2418

Wendel, A. (1981). Glutathione peroxidase. *Methods Enzymology*, *77*, 325–332. https://doi.org/10.1016/S0076-6879(85)13063-6

Wyse, A. T. S., Streck, E. L., Barros, S. V., Brusque, A. M., Zugno, A. I., & Wajner, M. (2000). Methylmalonate administration decreases Na^+, K^+-ATPase activity in cerebral cortex of rats. *Neuro Report*, *11*, 2331–2334. https://doi.org/10.1097/00001756-200007140-00052

Yousefi, S., Gold, J. A., Andina, N., Lee, J. J., Kelly, A. M., Kozlowski, E., … Simon, H. U. (2008). Catapult-like release of mitochondrial DNA by eosinophils contributes to antibacterial defense. *Nature Medicine*, *14*, 949–953. https://doi.org/10.1038/nm.1855

Zosky, G., R. , Janosi, T., Z. , Adamicza, A. , Bozanich, E., M. , Cannizzaro, V. , Larcombe, A., N. , et al. The bimodal quasi-static and dynamic elastance of the murine lung. *Journal of Applied Physiology* 2008;*105*, 685-692 https://doi.org/10.1152/japplphysiol.90328.2008

Zou, W., Ding, F., Niu, C., Fu, Z., & Liu, S. (2018). Brg1 aggravates airway inflammation in asthma via inhibition of the PI3K/Akt/mTOR pathway. *Biochemical and Biophysical Research Communications*, *18*, 3212–3218. https://doi.org/10.1016/j.bbrc.2018.08.127

How to cite this article: Silveira JS, Antunes GL, Kaiber DB, et al. Autophagy induces eosinophil extracellular traps formation and allergic airway inflammation in a murine asthma model. *J Cell Physiol.* 2019;1–14. https://doi.org/10.1002/jcp.28966